Journal of Optoelectronics and Advanced Materials Vol. 7, No. 5, October 2005, p. 2647 - 2654

# OPTICAL PROPERTIES OF $Ge_{20}Se_{80-X}Bi_X$ THIN FILMS

P. Sharma*, M. Vashistha[a], I. P. Jain[b]

Govt. Girls (PG) College, Sri Ganganagar–335001, Rajasthan, India.
[a]P.N.D. College, Gajsinghpur, Sri Ganganagar, Rajasthan, India
[b]Centre for non-conventional energy resources, University of Rajasthan, Jaipur-302004, India

In the present work the optical properties of Se substituted by Bi in $Ge_{20}Se_{80}$ thin films have been studied. Optical reflection and transmission spectra, at normal incidence of $Ge_{20}Se_{80-x}Bi_x$ thin films (x = 0,4,6,8,10,12) were obtained in the range 200 nm – 840 nm. The optical energy gap was estimated from the absorption coefficient values using Tauc's procedure. It is found that, the optical band gap decreases with increasing bismuth content. The extinction coefficient, refractive index, real and imaginary parts of the dielectric constants have been calculated.

(Received June 14, 2005; accepted September 22, 2005)

*Keywords*: Chalcogenides, Optical properties, Band gap, Germanium selenide, Optical constants

## 1. Introduction

Chalcogenide glasses represent one of the major categories of amorphous semiconductors because of their physical properties such as the switching and memory effects [1-4] and are well known for their IR transmittance [5,6]. These materials exhibit a wide range of photoinduced effects accompanied by significant changes in their optical constants, and applicable as optical recording or imaging media [7], absorption filters, laser fibre amplifiers, ultra low loss telecommunication links, radiation resistant telecommunication links, flexible $CO_2$ laser power guides [8], image bundles for detector array dissection, temperature, pressure and chemical sensors, non-linear components and many other optical elements [9,10]. Knowledge of the optical properties of these amorphous materials is obviously necessary for exploiting their very interesting technological potential. Optical and structural features of semiconductor films depend on the conditions of their preparation [11,12].

Optical properties are important in view of the intensive interest in the optoelectronic devices. Chalcogenide glassy semiconductors are generally p-type semiconductors and Bi - modified germanium chalcogenide glasses Ge-M-Bi (M = S, Se, Te) exhibit a p-n transition at high Bi concentration e.g., 11at % in Ge-S, 7at% in Ge-Se and 3.5 at% in Ge-Te [13]. In the present work a detailed investigation of optical properties of Se substituted by Bi in $Ge_{20}Se_{80}$ system have been undertaken.

## 2. Experimental

Bulk $Ge_{20}Se_{80-x}Bi_x$ materials (x = 0, 4, 6, 8, 10, 12) were prepared by the well known conventional melt quenching technique. The ingots so obtained were characterised for amorphicity by taking XRD patterns. Thin films of $Ge_{20}Se_{80-x}Bi_x$ were prepared at room temperature at $10^{-5}$ Torr vacuum using flash evaporation technique on a glass substrate of 1 cm × 1 cm size. The film thickness was kept around 2000A$^o$ which was measured by quartz crystal digital thickness monitor

* Corresponding author: pratibha_phy@sify.com

DTM –101 model. The samples were well characterized by taking XRD, DSC, EPMA and XRF [14].

In order to determine the absorption coefficient $\alpha$ and optical constants of the films as a function of the incident light wavelength, a measurement of the spectral transmittance $T(\lambda)$ and reflectance $R(\lambda)$ has been carried out at normal incidence in the wavelength range 200 nm – 840 nm by means of a Hitachi double monochromator spectrophotometer model 330.

## 3. Results and discussion

Study of the materials by means of the optical absorption provides a simple method for explaining some features concerning the band structure and energy gap of non metallic alloys [15]. The transmission and reflection spectra for $Ge_{20}Se_{80-x}Bi_x$ thin films were recorded in the wavelength range 200 nm to 840 nm. The absorption coefficient can be determined using the following relation

$$T= [(1-R)^2e^{-\alpha d}/1-R^2\ e^{-2\alpha d}] \quad (1)$$

where d is the thickness of the sample [16]. For many glassy and amorphous non-metallic materials, the absorption edge can be divided into two regions depending on the value of absorption coefficient $\alpha$.

(I) In case of $\alpha < 10^4$ $cm^{-1}$, there is usually an Urbach tail [17] in which $\alpha$ depends exponentially on photon energy, $h\nu$ as

$$\alpha = \alpha_o \exp(h\nu / E_e) \quad (2)$$

where $\alpha_o$ is a constant and $E_e$ is the width of the band tail of the localized states in the band gap also called Urbach slope. Fig. 1 shows the variation of $\ln\alpha$ with the photon energy $h\nu$. Variations in the width of the exponential region $E_e$, provide information about the relative changes of the structural disorder induced by an additive. For a good chalcogenide material, a typical value of the slope $E_e$ is around 50 meV. Tauc [19] believed that it arises from electronic transitions between localized states in the band edge tails; the density of which is assumed to fall off exponentially with energy. Davis and Mott were uncertain about the precise explanation of the exponential dependence and suggested that the slopes of the observed exponential edges obtained from above equation are very much the same in many semiconductors, and the value of $E_e$ for a range of amorphous semiconductors lie between 0.045 and 0.67 eV [18]. The values of $E_e$ calculated from figure 5 and using equation (2) are indicated in Table 1. The optical absorption edge was found to shift towards lower values of photon energies with increasing Bi content the reason could be shrinking of the energy gap [20, 21]. The edge value varies from 3.00eV for $Ge_{20}Se_{80}$ to 1.95eV for $Ge_{20}Se_{80}Bi_{12}$.

(II) In case of $10^4 \leq \alpha \leq 10^6$ $cm^{-1}$ in the high absorption region (where absorption is associated with interband transitions) Tauc [19] and Davis and Mott [22] independently derived an expression relating the absorption coefficient $\alpha$ to the photon energy $h\nu$

(III)

$$\alpha\, h\nu = \beta[h\nu - E_{g\,opt}]^n \quad (3)$$

where, $\beta$ is the band tailing parameter and is equal to

$$\beta = (4\pi\sigma / ncE_c), \quad (4)$$

where c is the speed of light and $\sigma$ is the minimum metallic conductivity(extrapolated d.c conductivity at $T = \infty$). $E_c$ is a measure of the width of the tail states distribution, n is the refractive index and $E_{g\ opt}$ is the optical band gap [23]. In the above equation n = ½ for a direct allowed transition, n = 3/2 for a direct forbidden transition, n = 2 for an indirect allowed transition and n =3 for an indirect forbidden transition. The study of the spectrum of the absorption coefficient $\alpha$ of a semiconductor in the fundamental region and near the fundamental edge provides us with valuable information about the energy band structure of the material.

Table 1.

| Composition | $E_e$(meV) | $\beta(cm^{-1}eV^{-1})$ | $E_g^d$ (eV) | $E_g^i$ (eV) |
|---|---|---|---|---|
| | | (x $10^5$) | | |
| $Ge_{20}Se_{80}$ | 25.9 | 1.61 | 2.14 | 1.49 |
| $Ge_{20}Se_{76}Bi_4$ | 28.4 | 2.19 | 2.09 | 1.46 |
| $Ge_{20}Se_{74}Bi_6$ | 34.4 | 1.94 | 1.95 | 1.45 |
| $Ge_{20}Se_{72}Bi_8$ | 38.3 | 2.45 | 1.80 | 1.29 |
| $Ge_{20}Se_{70}Bi_{10}$ | 47.5 | 1.42 | 1.79 | 1.25 |
| $Ge_{20}Se_{68}Bi_{12}$ | 54.8 | 2.39 | 1.69 | 1.17 |

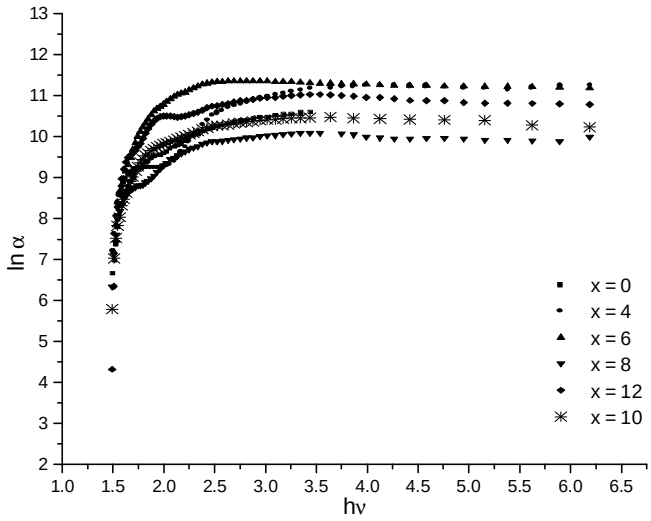


Fig. 1. Variation of logarithm of absorption coeffiecient with the incident photon energy.

For indirect and direct allowed transitions the energy gaps were determined by the intercept of the extrapolations to zero absorption with the photon energy axis are taken as the values of the indirect and direct energy gaps $E_g^i$ and $E_g^d$ respectively. Fig. 2 and Fig. 3 shows the variations of $(\alpha h\nu)^2$ and $(\alpha h\nu)^{1/2}$ vs. $h\nu$ respectively. The values of direct and indirect band gaps calculated from the graphs are listed in the Table 1 and the variation with incident photon energy $h\nu$ is shown in Fig. 8. It is clear from the figures that both direct and indirect band gaps decreases with increasing Bismuth content. The indirect band gap decreased from 1.48 to 1.16 eV and the direct band gap decreases from 2.14 to 1.68 eV when Bi content is increased from x = 0 to x = 12. Data listed in Table 1 reveals that the addition of Bi in the glass structure caused deeper band tails extended in the gap and thereby leading to a decrease in the value of optical band gap. The decrease of optical band gap with increasing Bi content is related to the increase of Bi-Se bonds and the decrease of Se-Se bonds. Bismuth enters into the tetrahedral structure $GeSe_2$ forming units containing all the three elements (Ge, Se, Bi) thus leading to the modification of the glassy network. Further, the optical band gap is strongly dependent on the fractional concentration of atoms. The decrease in the optical band gap is qualitatively in agreement with the concept that a decreasing ionic character of the covalent bond leads to a small energy gap of the corresponding material of the system. The lone pair electrons adjacent to Bi atoms will have higher energies than those remote from Bi atoms, causing a broadening and tailing of the lone-pair valence band of the chalcogen. This effect can account for the shallower slope $\beta$ with increasing Bi content.

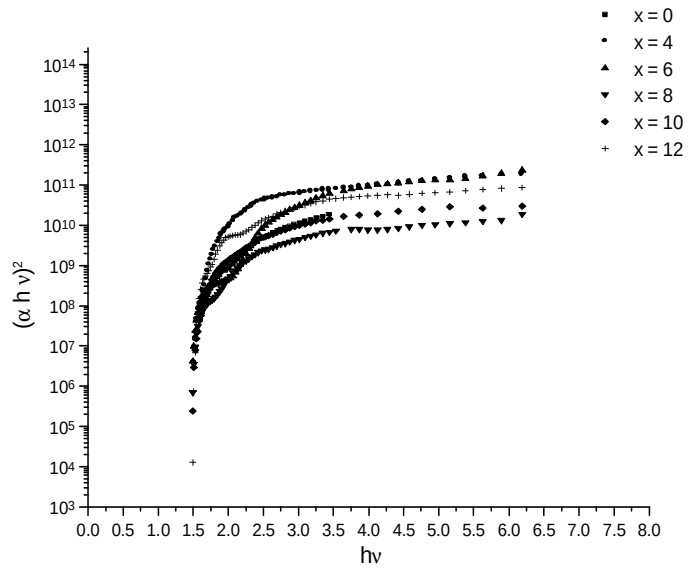


Fig. 2. Variation of $(\alpha h\nu)^2$ with hν for $Ge_{20}Se_{80-x}Bi_x$ thin film with x = 0, 4, 6, 8, 10, 12.

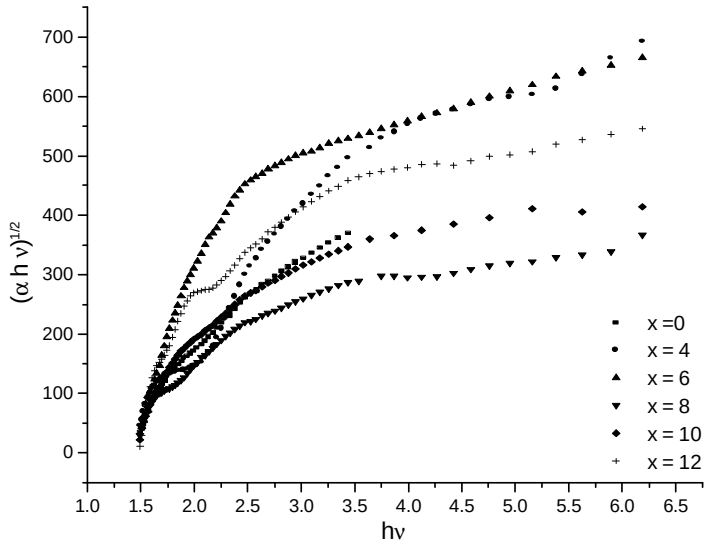


Fig. 3. Variation of $(\alpha h\nu)^{1/2}$ with hν for $Ge_{20}Se_{80-x}Bi_x$ thin film with x = 0, 4, 6, 8, 10, 12.

The slope of the curves $(\alpha h\nu)^{1/2}$ and $(\alpha h\nu)^2$ vs. hν gives the value of β which is a measure of the structural randomness the values so obtained from Fig. 2 and 3 are listed in Table 1 and the increase in the value of β with increase in the Bi content indicates the increase in the rigidity of the network and thus the modification in the network structure of the $Ge_{20}Se_{80}$ system [24].

From the absorption coefficient data extinction coefficient can be calculated

$$k = \alpha \lambda / 4\pi \quad (5)$$

Further the refractive index n can be calculated [22] using the relation:

$$R = [\{(n-1)^2 + k^2\}/\{(n+1)^2 + k^2\}] \quad (6)$$

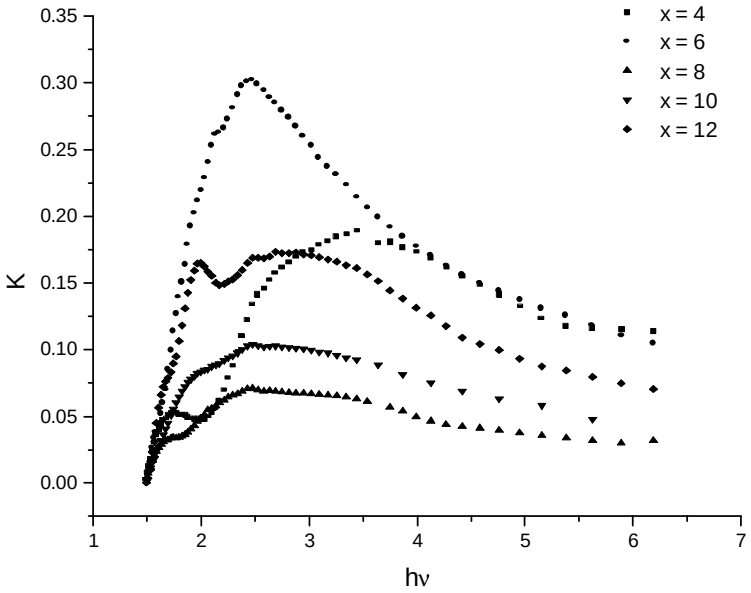


Fig. 4. Variation of extinction coefficient 'k' with the incident photon energy hν.

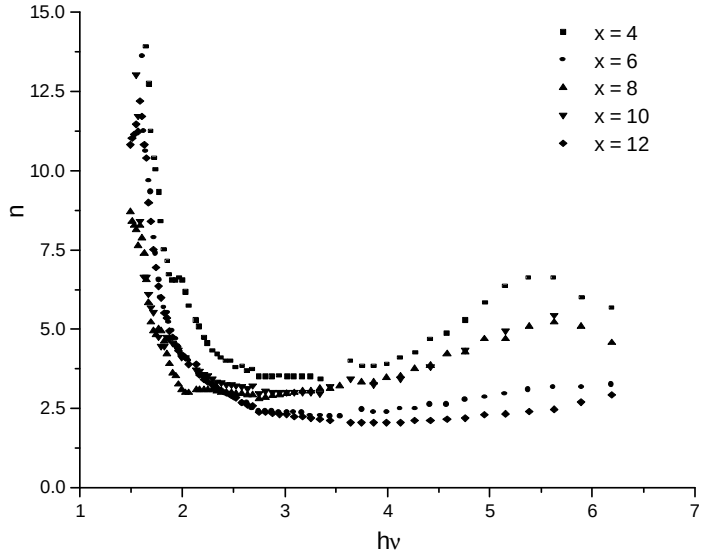


Fig. 5. Variation of refractive index 'n' with the incident photon energy hν.

Fig. 4 and 5 shows the variation of extinction coefficient k and refractive index n with the photon energy hν. From Fig. 4 it appears that the k curve shows a single broad peak for lower Bi content and another peak starts appearing with increasing Bi content and the peak position too was found to shift towards lower energy with increasing Bi content. While the value of n was found decrease with increasing photon energy for all films finally increasing slightly near 6 eV showing a small peak whose peak value decreases with increasing Bi content. The changes obtained in the

values of k and n are due to change in the stoichiometry [25], change in crystallite size [26] and internal strain [27] of the glassy alloy with Bi incorporation. While Fig. 6 and 7 show the real part $\varepsilon' = n^2 - k^2$ and the imaginary part $\varepsilon'' = 2nk$ of complex dielectric constant [28] variations with hν.

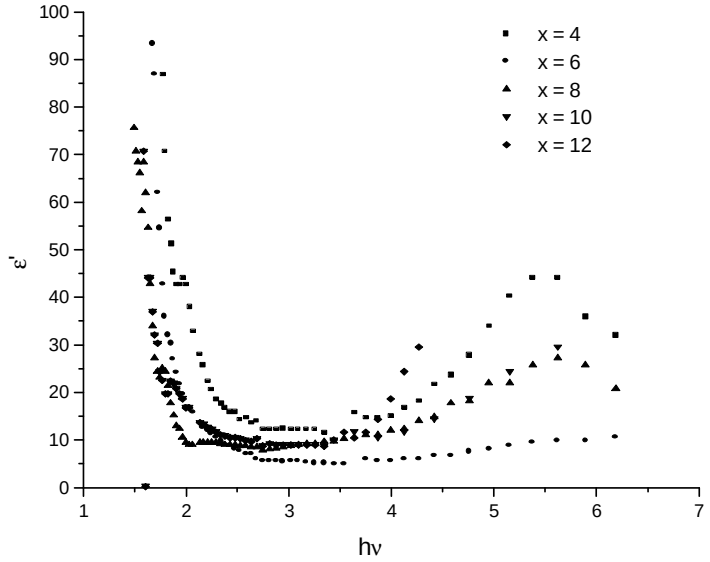


Fig. 6. Variation of real part of dielectric constant ε' with hν.

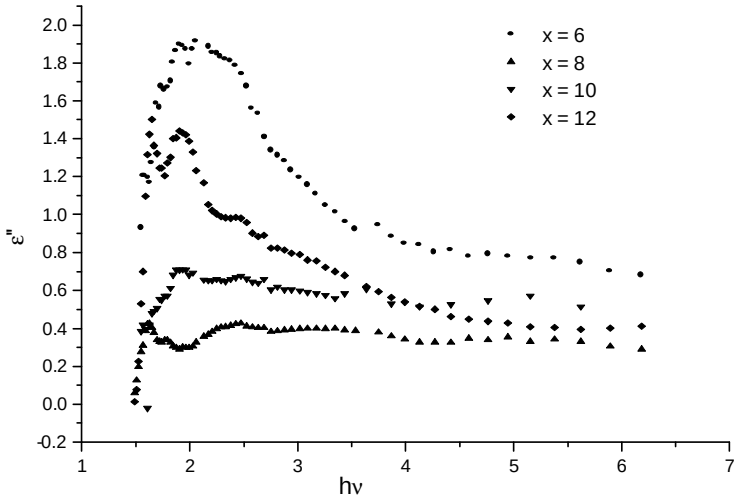


Fig. 7. Variation of complex part of dielectric constant ε" with hν.

The dispersion curves for the refractive index, real and the imaginary part of the dielectric constant reveal that the general behaviour of these constants are the same and show maximum near the absorption edge. From the Fig. 6 it appears that the variation of ε' with photon energy hν shows two peaks near 1.5 eV and 7 eV and that the peak value increases with increasing Bi content. ε" is directly related to the density of states within the forbidden gap of the amorphous semiconductor. Fig. 7 showing the variation of ε" with hν have a single broad peak and the peak value shifts towards higher energy with increasing Bi content. One more peak appears and becomes distinctly visible with increasing Bi content in ε" curve. two peaks which becomes clear and more distinct with the increasing Bismuth content. The ε" spectrum of most chalcogenides consists of two peaks below

10 eV, both of which survive disordering. The lower and higher energy peaks are frequently attributed to $\pi \rightarrow \sigma^*$ and $\sigma \rightarrow \sigma^*$ transitions respectively [29].

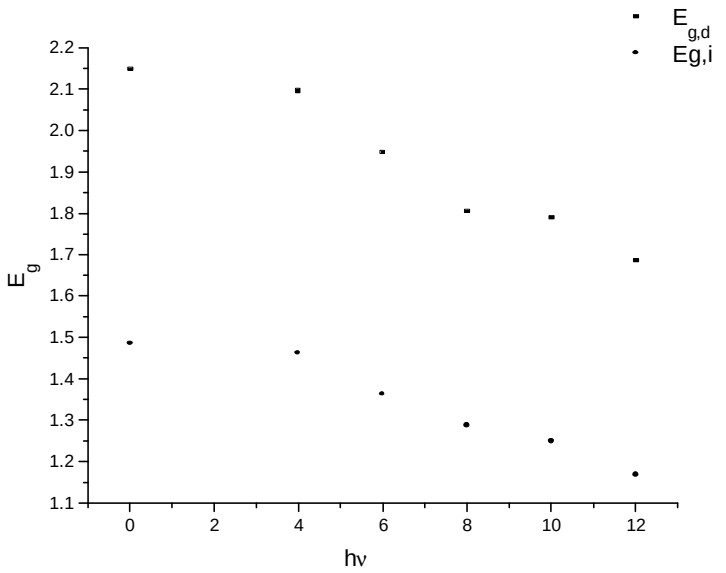


Fig. 8. Variation of direct $E_g^d$ and indirect band gap $E_g^i$ with hν.

## 4. Conclusions

The study of the optical properties of $Ge_{20}Se_{80-x}Bi_x$ thin amorphous films showed a distinct variation in the refractive index *n*, absorption coefficient α and the extinction coefficient *k* with the variation of Bi content. The more apparent phenomenon is the variation of optical band with variation of Bi content and it fits well with the equations 2 and 3. It was found that:

- The optical edge was found to shift towards lower values of photon energies with increasing Bi content the reason could be shrinking of the energy gap.
- The energy dependence of the optical absorption coefficient α is characterised by: (a) The values obtained for α were fairly high ($\alpha = 10^3 - 10^{12}$ $cm^{-1}$). (b) All the films exhibit two distinct absorption regions, a high energy threshold and another low energy threshold possibly corresponding to the two absorption mechanisms.
- The variation in the value of extinction coefficient k and refractive index n could be explained in terms of the changes introduced in the stoichiometry, crystalline size and internal strain of the glassy alloy due to the introduction of Bi.
- It was found that the ε' has two peaks while ε'' shows a single broad peak but another peak starts appearing with increasing Bi content and becomes distinctly visible at higher Bi concentration. The lower energy peak in ε'' spectrum corresponds to $\pi \rightarrow \sigma^*$ transitions while the higher energy peak to $\sigma \rightarrow \sigma^*$ transitions.
- The indirect band gap value was found to decrease from 1.48 to 1.16 eV and the direct band gap from 2.14 to 1.68 eV with increasing Bi content. This decrease in the both the optical band gaps with increasing Bi content is related to the increase in the localized state density within the band gap as suggested by Davis and Mott [22].
- The decrease in optical band gap with increasing Bi amount is also related to the increase of Bi-Se bonds and the decrease of Se-Se bonds.

**Acknowledgement**

Authors are thankful to SSPL New Delhi India for EPMA and Prof. Nirmal Singh of Physics Department Panjab University Chandigarh India for providing XRF technique. We are grateful to

the UGC, New Delhi, India for the financial support in the form of a minor research project. The authors are thankful to Dr. Y. K.Vijay of University of Rajasthan, Jaipur, India for providing the experimental facility.

## References

[1] D. L. Eaton J. Amer. Ceramic soc. **47**, 554 (1964).
[2] S. R. Ovshinsky Phys. Rev. Lett. **21**, 1450 (1968).
[3] K. W. Boer, S. R. Ovshinsly, J. Appl. Phys. **41**, 2675 (1970).
[4] H. S. Metwally Vacuum **345- 35**, 162 (2001).
[5] J. A. Savage, Infrared Optical Materials and their Antireflection Coatings, A. Higler, London 1985.
[6] D. Lezal, J. Optoelectron. Adv. Mater. **5**(1), 23 (2003).
[7] A. E. Owen, A. P. Firth, P. J. S. Ewen, Phil. Mag. B **52**, 347 (1985).
[8] X. Zhang, H. Ma, J. Lucas, J. Optoelectron. Adv. Mater. **5**(5), 1327 (2003).
[9] S. R. Elliot, Physics of Amorphous Materials, Longman, New York, 1990.
[10] P. Sharlandjev, B. Markova, J. Optoelectron. Adv. Mater. **5**(1), 39 (2003).
[11] M. M. El-Samanoudy, Thin Solid Films **423**, 201 (2003).
[12] P. Klocek, L. Colombo, J. Non-cryst. Solids **93**, 1 (1987).
[13] K. L. Bhatia, G. Parthasarathy, A. Sharma, E. S. R. Gopal, Phys. Rev. B **38**, 6342 (1988).
[14] Pratibha Sharma, M. Vashistha, I. P. Jain, Radiation Measurements **36**, 663 (2003).
[15] E-Abd El- Wahabb, Vacuum **57**, 339 (2000).
[16] A. Ashour, N. El – Kadry, S. A. Mahmoud, Thin Solid Films **269**, 117 (1995).
[17] F. Urbach Phys. Rev. 92: 1324 (1953).
[18] Abdelghany A, Elsayed S. N., Abou El Ela A, Mousa NH. Vacuum **47**, 243 (1996).
[19] J. Tauc, in: F. Abeles (ed.) Optical properties of solids, North Holland, Amsterdam, 1970, p. 903.
[20] J. Sottropoulos, N. Fuhs, J. Non-Cryst. Solids **114**, 97 (1989).
[21] K. L. Bhatia, V. K. Bhatnagar, J. Non-Cryst. Solids **104**, 17 (1988).
[22] E. A. Davis, N. F. Mott, Philos. Mag. **22**, 903 (1970).
[23] K. L. Bhatia, S. Fabian, S. Kalbitzer, Ch. Klatt, W. Kratschmer, R. Stoll, J. F. P. Sellschop, Thin Solid Films **324**, 11 (1998).
[24] A. Masuda, Y. Yonezawa, A. Morimoto, M. Kumeda, T. Shimizu, J. Non-Cryst. Solids **217**, 121 (1997).
[25] K. Yamaguchi, N. Nakayama, H. Matsumoto, S. I. Kegami, Jpn. J. Appl. Phys. **16**, 1203 (1977).
[26] F. Tepehan, N. Ozer, Solar Energy Mater. Solar Cells, **30**, 353 (1993).
[27] A. Ashour, N. El-Kdry, S. A. Mahmoud, Thin Solid Films **269**, 117 (1995).
[28] H. A. Zayed, Thin Solid Films **274**, 128 (1996).
[29] J. Robertson, Advances in Physics **32**(3), 361 (1983).